Design for Scientific RENAISSANCE

JASER

Calcium Carbonate Crystals Formation by Ureolytic Bacteria Isolated from Australian Soil and Sludge

Salwa Al-Thawadi[1,a], Ralf Cord-Ruwisch[2,b]

[1]University of Bahrain, Department of Biology, Sukhir, Kingdom of Bahrain.

[2]School of Biological Sciences and Biotechnology, Murdoch University, Perth, WA, Australia.

[a]salthawadi@sci.uob.bh, [b]cord@murdoch.edu.au

Article Info

Received: 10th October 2011
Accepted: 5th January 2012
Published online: 1st March 2012

ISSN 2231-8844

ABSTRACT

Ureolytic bacteria were isolated selectively from sludge and soil samples (Perth, Western Australia). Three isolates were genetically examined by 16S rRNA. They were mostly closely related to Bacillus species. A bacterium producing the highest urease activity, Bacillus sp. MCP11 (DSM 23526), was used to precipitate calcium carbonate crystals. These crystals were precipitated due to bacterial activity in the presence of cementation solution (urea and calcium chloride, up to 1 M). Ureolytic bacteria hydrolyse urea producing carbonate and NH_4^+ causing an increase in the pH. In the presence of calcium ions in excess, calcium carbonate will precipitate. Type, size and shape of the precipitated calcium carbonate crystals were characterized by using light microscope and Scanning Electron Microscope (SEM). It was found that vaterite (spheres) and calcite (rhombohedral crystals) were precipitated at the surface of sand granules indicating the possibility of using those crystals to cement loose sand.

Keywords: calcite; cementation; SEM; ureolytic bacteria; vaterite

1. Introduction

Calcium carbonate ($CaCO_3$) is widely distributed mineral in nature. It can form loose crystals from rapid chemical reaction of carbonate and calcium ions. However its precipitation can also be triggered by bacterial reactions. Bacterial $CaCO_3$ precipitation under appropriate conditions is a general phenomenon occurring in nature (Boquet et al., 1973).

There are a number of species of $CaCO_3$ minerals associated with bacteria, for example vaterite formation by Acinobacter sp. (Sanchez-Moral et al., 2003), aragonitic sherulites by Deleyahlophila (Rivadeneyra et al., 1996), calcite by E. coli (Bachmeier et al., 2002) and magnesium calcite spherulites and dumbbells by the slime-producing bacteria, Myxococcus xanthus (Holt et al., 1993; González-Muñoz et al., 2000).

The $CaCO_3$ precipitation rate in general is a linear function of the concentration of the ion products, Ca^{2+} and CO_3^{2-} (Longdon et al., 2000) hence obeying 2nd order kinetics or 1st order kinetics if one of the reactants (e.g. calcium) is in excess. The microorganisms can influence the attainable saturation and the rate of $CaCO_3$ precipitation, controlling the polymorph of the produced $CaCO_3$ crystals (Bosak et al., 2004; Bosak and Newman 2005). When the

concentration of Ca^{2+} and CO_3^{2-} exceeds the solubility product (K_{sp}), supersaturation of solution is reached (Eq. 1). The higher the supersaturation index (SI) is the more likely precipitation of $CaCO_3$ is to take place. The saturation index (SI) of a solution with respect to $CaCO_3$ is defined by:

$$SI = \frac{\left[Ca^{2+}\right]\left[CO_3^{2-}\right]}{K_{sp}} \quad (1)$$

Where $[Ca^{2+}]$ $[CO_3^{2-}]$ represent the ion activity product (IAP) and K_{sp} is the calcite solubility product.

One particular process by which significant amounts of calcite can be formed rapidly is by the bacterial release of carbonate from the hydrolysis of urea in the presence of calcium solution. In fact, an equi-molar mixture of urea and calcium chloride solution can be considered as a cementation solution. In the presence of this cementation solution, ureolytic bacteria will form $CaCO_3$ crystals at controllable rates and NH_4^+ ions which cause the pH to increase (Eq. 2).

$$CO(NH_2)_2 + Ca^{2+} + 2\,H_2O \xrightarrow{\text{Urease}} 2NH_4^+ + CaCO_3 \quad (2)$$

Ferris et al. (2004) revealed that the ureolytic bacteria (Sporosarcina pasteurii) precipitate $CaCO_3$ crystals by generating carbonate from urea hydrolysis with the crystal formation occurring in three different stages: (1) The development of supersaturated solution, (2) Nucleation at the point of critical saturation (i.e. the supersaturation at which $CaCO_3$ actually initiates), and (3) Spontaneous crystal growth on the stable nuclei.

It seemed worthwhile to examine microbiologically formed $CaCO_3$ crystals (type, shape and size) at the micro scale, as the crystals are critical for in-situ biocementation and possibly other processes. This study aims at determining the morphology and types of $CaCO_3$ crystals which were precipitated in the presence of high concentrations of cementation solution (calcium/urea) and produced by ureolytic bacterial cells. Different sizes of $CaCO_3$ crystals may be necessary for different applications. For example, larger crystals are more useful to cement coarse sand. Thus, this study aims at examining the size of $CaCO_3$ crystals formed at different concentrations of cells and cementation solution.

2. Materials and Methods

2.1 Enrichment, Isolation and Identification of Highly Ureolytic Bacteria

Potential microbial calcite precipitating bacteria with high urease activity (mM urea hydrolysed.min^{-1}, measured by conductivity), specific activity (mM urea hydrolysed.min^{-1}.OD^{-1}, the amount of urease activity per unit biomass at OD_{600} nm) and stability were enriched from different locations (activated sludge from a wastewater treatment plant (Woodman Point, Perth, Western Australia)), and soil from manure fertilised fields and

surrounding cattle stables (Veterinarian Farm, Murdoch University, Perth, Western Australia). One gram of soil or sludge was placed in 50 ml of growth media (250 ml shaking flasks, at 28^{o}C, for 36 hours). The enrichment medium consisted of 10 g.L^{-1} Yeast extract (YE), 1-5 M urea, 152 mM ammonium sulphate and 100 mM sodium acetate.

To screen for pure colonies, the enrichment cultures were diluted and plated out on Nutrient Agar plates (NA, pH 7). NA contained 8% of filter sterilized urea which was added after the autoclaving. The plates were incubated at 28^{o}C for 48 hours. Filter sterilized phenolphthalein drops (indicator for the increase in pH caused by urease activity) were placed on the surface of the colonies and the change in the colour was recorded. After urea hydrolysis, the pH will increase up to 9.0 then a pinkish colour will surround the ureolytic bacteria. The individual colonies that showed a pinkish colour were individually transferred to a liquid medium similar to the enrichment medium, and were treated under the same conditions of enrichment cultivation.

Total genomic DNA from pure cultures (5 ml of MCP1, MCP4 or MCP11) was extracted using ultra clean™ soil DNA kit (Mo-Bio Laboratories Inc., CA). The extracted DNA was used in PCR amplifications to target the bacterial 16S rRNA gene using eubacteria-specific primers designed by (Muyzer et al., 1993). PCR amplification was initiated by denaturation at 95^{o}C for 10 min and was followed by 40 cycles of denaturation (95^{o}C, 30s), annealing (55^{o}C, 15s) and then by extension (72^{o}C, 30s). A final extension was carried out at 72^{o}C for 3 min. PCR products were separated by electrophoresis in 1.2% agarose gels, stained with ethidium bromide and visualized on a UV trans-illuminator. PCR products were purified using a Qiagen PCR purification kit (Qiagen, Australia). Nucleotide sequences of the PCR products were determined using the same primers, and the ABI-PRISM BigDye terminator V 3.0 cycle sequencing kit (Perkin Elmer) using an ABI-Capillary DNA sequencer (Perkin Elmer) at the State Agricultural Biotechnology Centre (SABC) at Murdoch University. Sequencing was carried out in duplicate. Putative identification of each sequence was carried out using Basic Local Alignment Search Tool (BLAST) (Altschul et al., 1990).

For all calcium carbonate precipitation experiments which were conducted in this study, Bacillus sp. MCP11 (DSM 23526) was used because it showed the highest urease and specific urease activities.

2.2 Calcium Carbonate Precipitation by Ureolytic Bacteria

Bacillus sp. MCP11 (DSM 23526, urease activity 1–2.8 mM urea hydrolysed.min^{-1}) was mixed with cementation solution to a final concentration of 1 M (equimolar of calcium/urea solution, calcium supplied as $CaCl_2.2H_2O$) in a microcentrifuge tube. The final urease activity on the microscopic slide was 0.6–1.6 mM urea hydrolysed.min^{-1}. Immediately, 20 µl of this mix were placed on a microscopic slide and then covered with a coverslip.

In the case of testing the ability of $CaCO_3$ to precipitate on sand granules, 200 mg silica sand granules (9 µm diameter) were placed on a microscopic slide. Then, 20 µl of the cementation mix (bacterial culture and cementation solution) were placed at the surface of the sand granules. To avoid the drying of the sample on the microscopic slide, the edges of the coverslip were sealed with nail polish. $CaCO_3$ crystal formation was examined (immediately and after 24 hours) by a compound microscope (BX51) fitted with a DP70 Digital Camera.

One week later, the samples were subjected to Scanning Electron Microscope (SEM) examination (SEM- Philp XL20). Energy Dispersive X-ray Microanalysis of $CaCO_3$ crystals was carried out using Oxford ISIS-5175 micro-analyser.

2.3 SEM Sample Preparations

Subsequent to growing $CaCO_3$ crystals on a microscopic slide covered with a coverslip, parts of the coverslip were placed on aluminium stubs using "Carbon Tabs" (ProSciTech, Queensland, Australia). The stubs were then placed in a dust proof container and allowed to dry completely at room temperature, overnight before being coated with a 20 nm layer of Gold in a Balzers Union Ltd. "sputter coater". SEM samples for X-ray analysis were not coated with gold but otherwise treated the same way.

2.4 The Effect of Different Concentrations of Bacterial Cells on the Size of the Calcium Carbonate Crystals Formation

Biocementation experiments on microscopic slides were carried out for the non-diluted bacterial culture (urease activity of 3.3 mM urea hydrolysed.min^{-1}, specific urease activity of 1.3 mM urea hydrolysed.min^{-1}.OD^{-1}, dry weight 30 g.L^{-1}) and for three different dilutions (3, 0.3, and 0.03 g.L^{-1}). The culture was diluted by a sterile saline solution to reach the desired dilution factor. During the biocementation experiment as mentioned previously, all the samples were further diluted almost twice. After 24 hours of $CaCO_3$ precipitation, the crystals were examined under the light microscope and the averages of different spheres sizes (5 spheres) were measured in average of 8 individual fields of focus.

2.5 The Effect of Different Concentrations of Cementation Solution on the Size of the Calcium Carbonate Crystals Formation

Biocementation experiments on microscopic slides were carried out using different concentrations of cementation solution (10-1250 mM equivalent concentration of calcium/urea). The sizes of the $CaCO_3$ spheres were measured by Image-Pro Express software from Media Cybernetics.

3. Results

3.1 Enrichment, Isolation and Identifying of Ureolytic Bacteria

To screen for ureolytic bacteria, it is necessary to select the conditions at which these types of microbes grow and produce urease. For a selective enrichment medium for ureolytic bacteria, the presence of urea as a substrate and an alkaline pH ($\geq$ 9.0) was necessary. After initial incubation of the selective enrichment; different levels of urease activity were obtained, ranging from 2-42.2 mM urea hydrolysed.min^{-1} (Appendix A).

The primary enrichments described above were transferred repeatedly to a fresh medium and then plated out on urease agar plates. Different ureolytic colonies were obtained. The most ureolytic active colonies could be spotted from pH increases in the agar medium indicated by a colour change to pink by Phenolphthalein. The medium becomes alkaline and

turns pink due to the presence of NH_3/NH_4^+. Thus this pH increase was used as an indicator of bacterial urease activity.

A number of different pure bacterial isolates were obtained (Appendix B) according to the previously described method. The common features of the three most suitable strains for biocementation process were as follows: Rod shaped cells that were characterized by the following features: Between 1-5 μm long, endogenous of urease production (i.e. after precipitating the cells by centrifugation, it was found that urease activity was only in the precipitate and not supernatant), fast growing (doubling time of 0.5-2.0 hours), highly tolerant to 1 M urea and 2 M ammonia, spore forming, relatively high urease activity (> 3.3 mM urea hydrolysed.min^{-1}).

PCR amplification of 16S rRNA was performed for three isolates (MCP1, MCP4 and MCP11). By blasting this sequence at NCBI (GeneBank), it was found that the isolates were closely related to a Bacillus species (All of the isolates were 99% related to Bacillus species CPB2, 96% related to B. aqamarinus, and 96% related to B. pasteurii.

3.2 Microscopic Examination of Calcium Carbonate Precipitation (Light Microscope)

It was particularly interesting to visualise the initial crystal formation which is assumed to be caused by oversaturation of $CaCO_3$ in the presence of adequate nucleation sites. Within minutes from the initiation of the biocementation process, spherical $CaCO_3$ deposits started to precipitate. These spheres were mostly clustered together in aggregates of two or more (Fig. 1A; Fig. 1B), while some were compacted forming non-spherical aggregates (Fig. 1C). The spheres were similar in size (Fig. 1C) in one field of focus (around 22 μm in diameter), while different (100-400 μm in diameter) in another field (Fig. 1D).

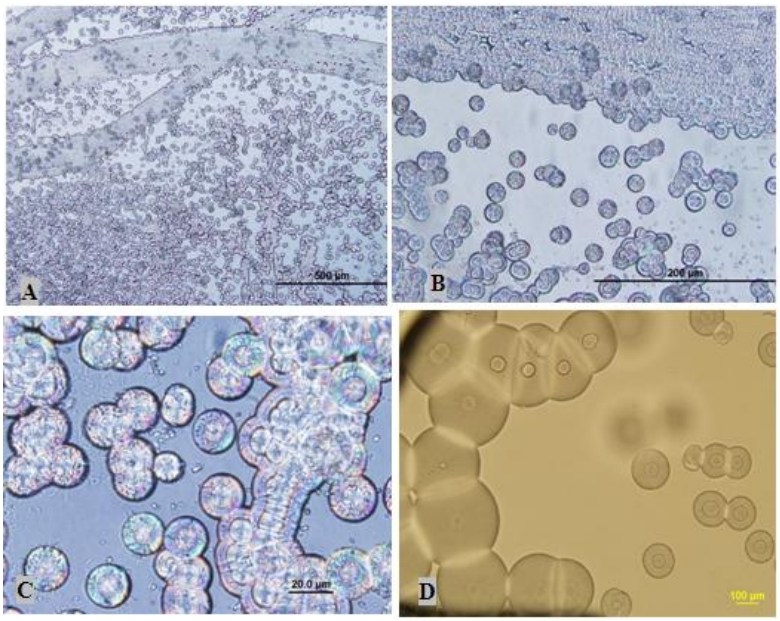

Fig.1. Light microscopic images of similarly sized (around 22 μm) bacterial $CaCO_3$ spheres at (A) 10X (overview), (B) 40X and (C) 100X (enlarged image) (D) and different sized (100-400 μm) at 100X (in another field of focus).

It was found that rhombohedral crystals appeared at a later stage of biocementation process (after 9 hours) as shown in Fig. 2.

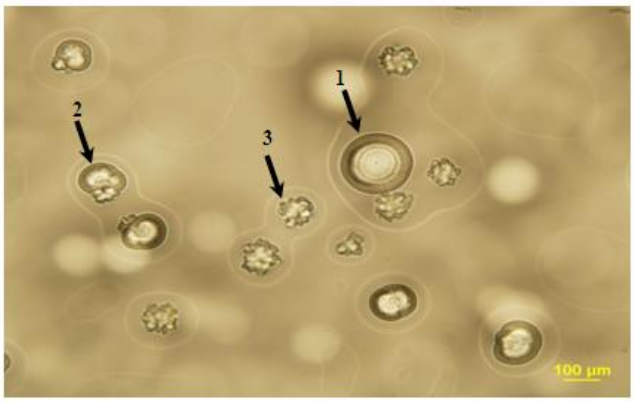

Fig.2. Light microscopic image showing three steps of producing the rhombohedral crystals from the spheres by the isolate MCP11. Where (1) illustrates the intact sphere, (2) illustrates part of the rhombohedral crystals appears from the spheres and (3) illustrates the rhombohedral crystals in a spherical arrangement were free without shell

3.3 Calcium Carbonate Crystals Examined by Scanning Electron Micrographs (SEM)

3.3.1 The Nature of Calcium Carbonate Precipitation

When using SEM, both spherical and rhombohedral crystals in spherical arrangements were observed in samples after about 1 week of initiation of the cementation reaction (Fig. 3). Energy Dispersive X-ray (EDS) revealed that both crystal types were composed of $CaCO_3$ (Fig. 4).

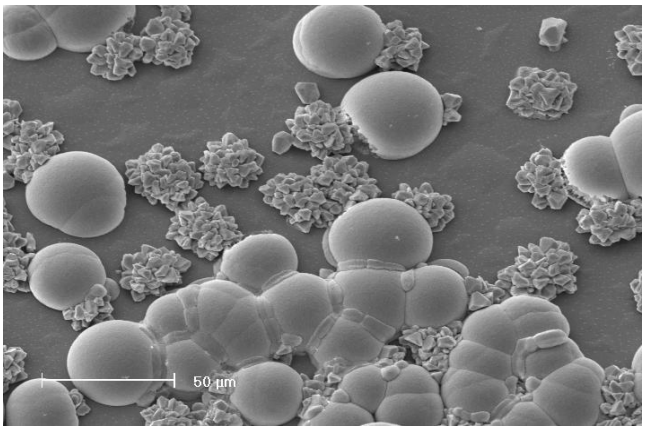

Fig.3. SEM image of (a) spherical and (b) rhombohedral $CaCO_3$ crystals after 1 week from the progress of cementation reaction using MCP11 with urease activity of 1.6 mM urea hydrolysed.min^{-1}

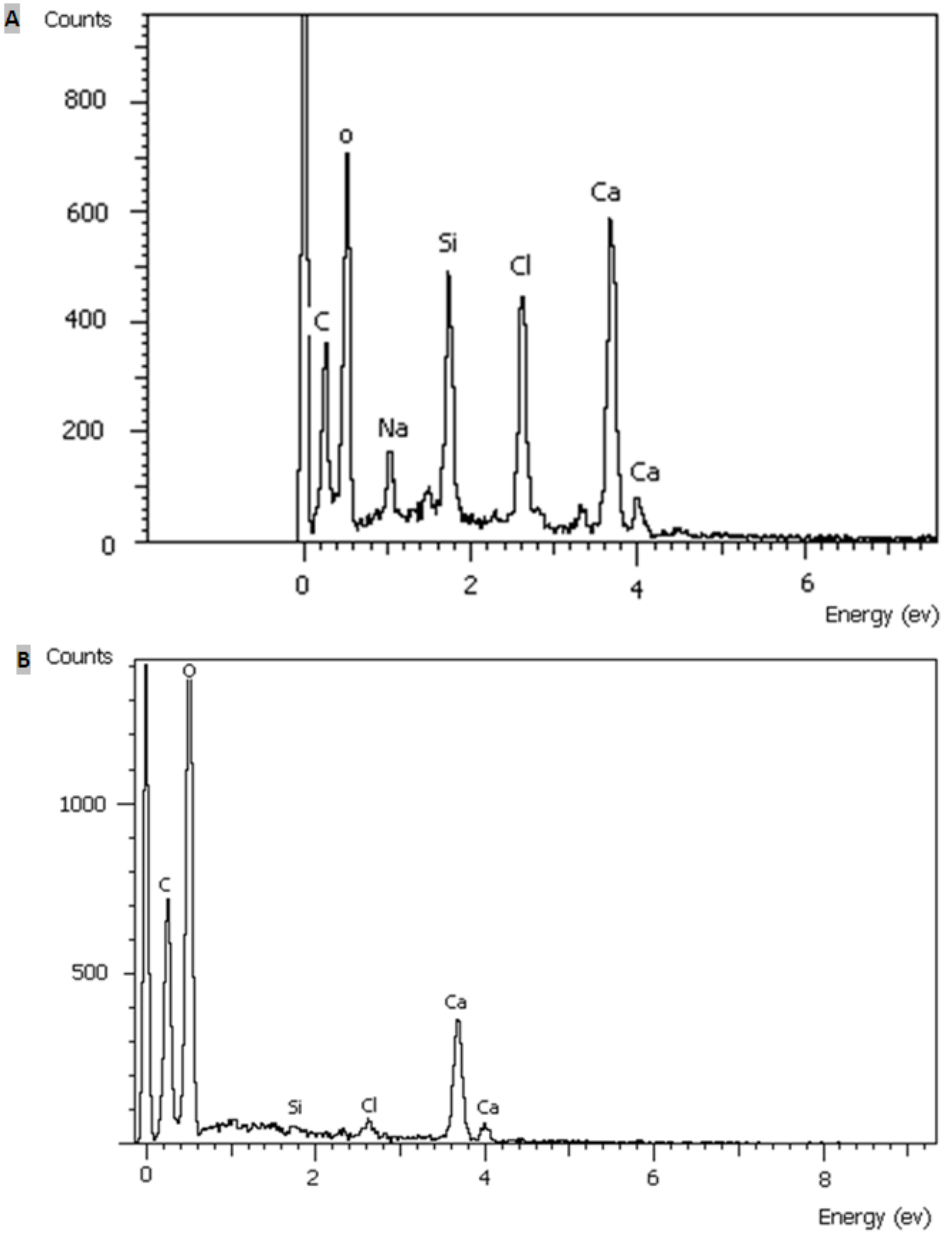

Fig.4. Energy dispersive X-ray spectroscopy (EDS) of bacterially induced $CaCO_3$ crystals using SEM-SiLi detector, those spectra indicate Ca peaks associated with the spherical (A) and rhombohedral (B) calcite crystals. Peaks for Si, Cl and Na originated from the glass, cementation solution and the culture medium respectively

It was a general observation that initially spherical crystals were formed, which did not persist. With increasing time course of crystal formation rhombohedral crystals formed as the final crystal form while the spherical crystals gradually disintegrated, which could be seen on a number of SEM micrographs (Fig. 3; Fig. 5; Fig. 6). XRD analysis of $CaCO_3$ which was precipitated by MCP11 under similar condition followed by this study; shows that vaterite and calcite crystals were formed (personal communication with L. A. Van Paassen). In addition, the observed meta-stable nature of the spheres, and their spherical shape (Braissant et al., 2003) suggests that the spherical $CaCO_3$ precipitate was vaterite. This suggestion has been supported by XRD analysis showing that $CaCO_3$ crystals (spheroids) which form at the beginning of the reaction between concentrated sodium carbonate and calcium nitrate were

vaterite (Andreassen and Hounslow, 2004). According to literature, the rhombohedral crystals with cubic faces are typical of calcite which has been supported by XRD analysis (Guo et al., 2003; Söllner et al., 2003).

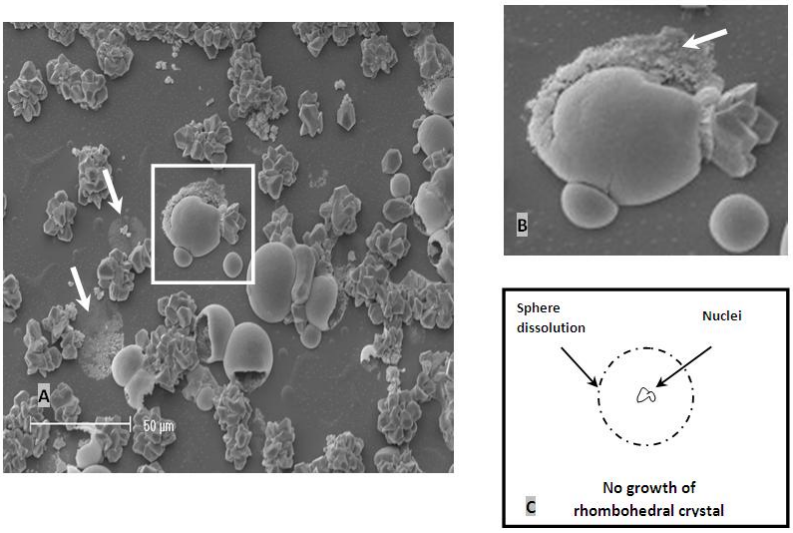

Fig.5. SEM micrographs of decomposed spherical $CaCO_3$ produced by MCP11 (final urease activity of 1.6 mM urea hydrolysed.min^{-1}). It seems that the spherical shell after certain time from being intact, dissolute gradually (arrows in A and B). (C) A schematic diagram of the degenerated spherical crystals that failed to produce rhombohedral crystals pointed with arrows in (A).

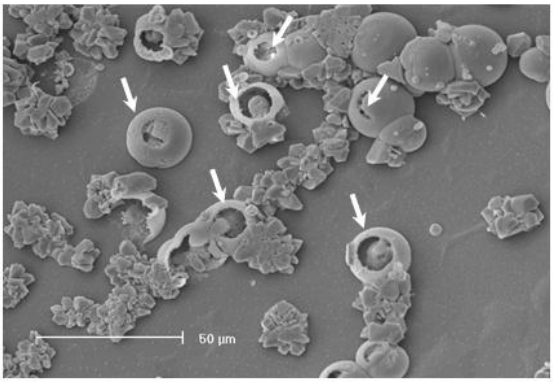

Fig.6. SEM image of the structured openings at the upper surface of the spherical $CaCO_3$ (see arrows) produced by MCP11 (final urea activity 1.6 mM urea hydrolysed.min^{-1})

3.3.2 Surface Texture of Calcium Carbonate Precipitation

The outside surface texture of the spheres was smooth with occasional openings of the more mature crystals (Fig.5). The thickness of the spherical wall varied between 4 µm and 0.08 µm. In more advanced stages, presumably during the phase of dissolution of the meta-stable vaterite crystals, some appeared to be hollow (Fig. 5) and others with signs of internal re-crystallisation (Fig.6). The differences may be due to different stages of the sphere development and possible transformation into the rhombohedral crystals.

The spherical crystals were able to cover the surface of the sand granules, connecting them together (Fig.7) and providing one mechanism for strength formation (i.e. bridging between the sand granules by $CaCO_3$ crystals was the mechanism which led to strength formation).

The concept of initial crystallisation of vaterite as reported in the literature, followed by re-crystallisation into calcite is not new (Ogino et al., 1987; Donners et al., 2002) but was observed in a very pronounced way during the described biologically induced calcium carbonate precipitation. It makes sense on the basis of the solubility products of vaterite ($ks=10^{-7.91}$, at 25^oC) and calcite ($ks=10^{-8.48}$, at 25^oC), such that simple modelling (data not shown) would predict that while the dissolved calcium carbonate concentration exceeds the saturation level for vaterite formation, vaterite is formed while at a later stage the lower solubility product of calcite draws calcium and carbonate ions from equilibrium, causing continued vaterite dissolution. In our experiments it was typically observed that all vaterite had disappeared and only rhombohedral calcite crystals remained when the reaction was allowed to complete under submerged conditions.

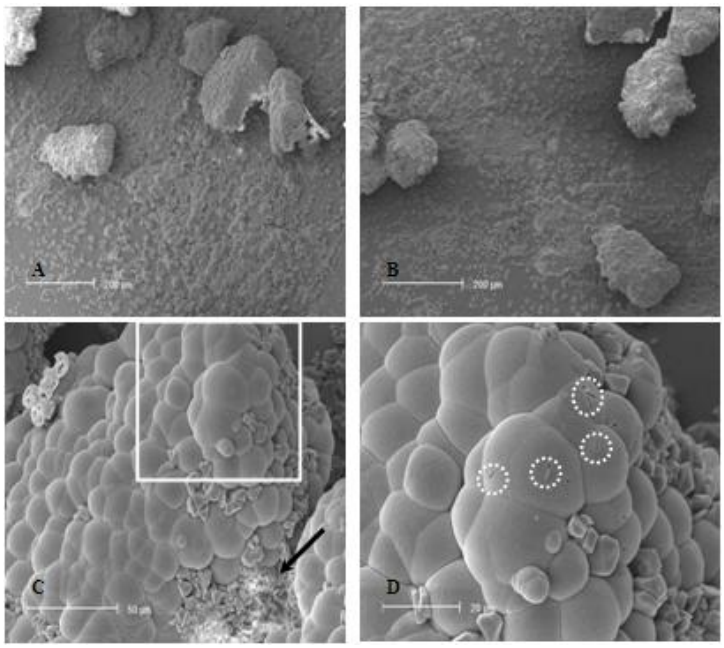

Fig.7. SEM micrographs of $CaCO_3$ crystals embedded on the coverslip and attached to 100-200 µm silica sand granules (A-D). The sand granules were fully covered by spherical $CaCO_3$ produced by MCP11. The dashed circles in D show the signs of bacterial cells (~1 µm) surface at the surface of the spherical $CaCO_3$

On some vaterite crystals, imprints of the bacterial cell-shape at the surface of the spherical crystals (Fig. 7D) could be observed, which is in line with the meta-stable nature of this mineral. Possibly it could be caused by a different chemical microenvironment around the bacterial cell either solubilising vaterite or preventing its formation. In contrast the presence of similar imprints at the surface of the rhombohedral crystals (Fig. 3; Fig. 5; Fig. 6) was never found.

3.4 The Effect of Different Concentrations of Bacterial Cells on the Size of the Calcium Carbonate Crystals

Based on the assumption that each vaterite crystal is formed by one bacterial cell, it was expected that by using lower bacterial concentrations, fewer but bigger spheres would be produced. However, results showed that the average size of sphere increased with the increase in bacterial cells concentration and hence urease activity (Fig. 8). If indeed the size of vaterite crystals increases with an increase in the rate of carbonate production, then the concentration of bacteria used (and hence of urease activity present) could be a useful control parameter for the production of crystals of designed size. For example in more coarse sands larger crystals would be expected of more benefit than in finer sands.

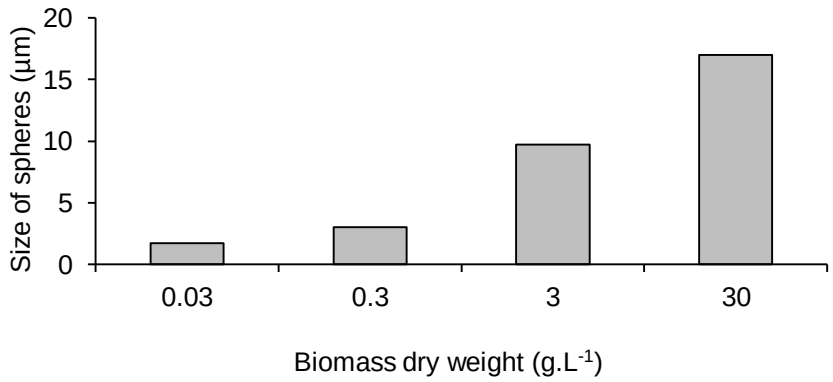

Fig.8. Different sizes of $CaCO_3$ crystals (spheres) produced by different concentrations of cells (MCP11).

3.5 The Effect of Different Concentrations of Cementation Solution on the Spherical Calcium Carbonate Crystals

The average size of the spheres increased as the concentration of the urea and calcium ions increased (Fig. 9). There was a sharp increase in the spherical size at concentrations of 10-250 mM above which the increase in the size was limited. Considering that the urease enzyme of the organisms tested shows a very high apparent half saturation constant (Km value), making the rate largely dependent on the urea concentration, is again the rate at which carbonate is produced that seems to control the crystal sizes, with smaller crystals only formed when the reaction rate is known to significantly slow (less than 300 mM).

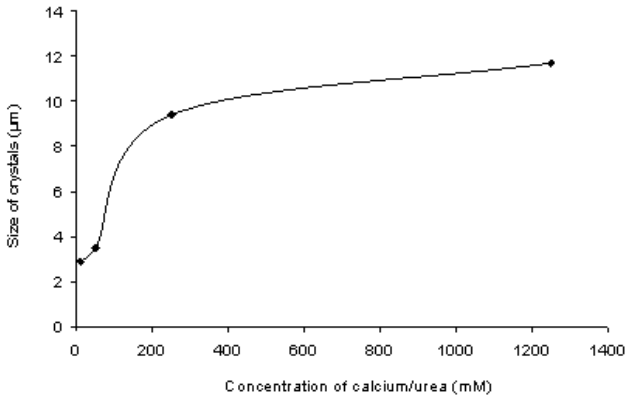

Fig.9. Different sizes of $CaCO_3$ crystals (spheres) produced by MCP11 in the presence of different concentrations of cementation solution (equimolar concentration of calcium/urea). Lowest concentration of calcium/urea tested was 10 mM.

4. Discussion and Conclusions

4.1 Enrichment, Isolation and Identifying Ureolytic Strains

Methods to enrich and isolate Bacillus bacteria from most soil within a short cultivation period were developed. These methods were designed to select ureolytic bacteria which were suitable for biocementation condition (high pH and tolerance to high concentration of ammonium ions) and which were superior to the existing strain of S. pasteurii. The high level of urease activity observed in some of the enrichment trials combined with the fact that urease activity was the key factor for successful biocementation, demonstrated that the enrichment culture can be used for biocementation process under high concentration of calcium/urea without the need of purification. Purification of cells is time consuming, laborious and costly process. Therefore, using enrichment cultures in the biocementation process could be more practical and cost effective.

Urease activity of the successfully isolated strains throughout this study was consistent. Accordingly, there was no problem encountered with the consistency of urease activity production as compared to the use of S. pasteurii in sand consolidation (Whiffin, 2004).

4.2 Calcium Carbonate Formation by Ureolytic Bacteria

As a general phenomenon, ureolytic bacteria in the presence of high concentration of calcium and urea produce two types of $CaCO_3$ precipitations; spherical deposits and rhombohedral crystals. Both spherical deposits and rhombohedral crystals were observed in one study addressed the removal of waste cations e.g. Sr^{2+} (Warren et al., 2001). Rhombohedral calcite crystals due to ureolytic bacterial activity in the absence of the spherical deposits were observed in other studies (Bang et al., 2001; Bang and Ramakrishman, 2002; Mitchell and Ferris 2006). There was no sign of cells at the surface of rhombohedral calcite crystals, which indicates that these types of crystals were chemically precipitated at high level of supersaturation. So the spherical localized area may form the

suitable conditions of supersaturation and alkalinity that enable $CaCO_3$ to precipitate. This alkaline localized area close to the cell surface is suggested to be due to active movement of calcium ions through Ca^{2+}/2H Pump (Hammes and Verstraete 2002). The chemical precipitation of rhombohedral crystals was described by Warren and his colleagues (2001). They did not observe embedded cells (S. pasteurii). In contrast, other authors noted that S. pasteurii embedded in the rhombohedral crystals indicating a direct involvement of the cells in the formation of the rhombohedral crystal (Bang et al., 2001).

Rhombohedral calcite crystals nucleate through self-assembly process which requires the combination of calcium cation and carbonate anion (Guo et al., 2003). The actual mechanism of the formation of those rhombohedral crystals from the spheres remains still unclear. However; in the literature similar observations of agglomerates of rhombohedral calcite was found at pH of 8.5 (Tai and Chen 1998) and super-saturation index of 30-40 (Dittrich et al., 2003).

The meta-stable behaviour of the microbial spherical $CaCO_3$ crystals supports the assumption that they may be suitable to be used as a template to encapsulate certain micro and macro-molecules. Suckhorukov and his colleagues (2004) have successfully chemically prepared decomposable, spherical, porous calcite crystals with an average size of 5 μm to be used for the encapsulation of biomolecules mainly proteins. Those spheres were suitable to enclose biomolecules due to their high surface area, the presence of nano-pores and channels in the spherical shell. Lactoalbumin and Ibuprofen (IBU) drugs were encapsulated in polyelectrolyte calcium carbonate microcapsule (Wang et al., 2006). IBU encapsulated $CaCO_3$ microparticles had a faster release in the gastric fluid more than the exposed IBU crystals. Further knowledge of what controls the size of such spheres could be useful for the development of vaterite immobilised biomolecules.

Acknowledgement

Authors wish to acknowledge the financial support given by University of Bahrain for this work. Authors as well would like to express their sincere appreciation to Gordon Thomson (Histology lab, Murdoch University, Australia) for his technical assistance in Olympus microscopic and SEM examinations.

References

Altschul, S. F., Gish, W., Miller, W., Myers, E. W., & Lipman, D. J. (1990). Basic local alignment search tool. Journal of Molecular Biology, 215, 403–410.

Andreassen, J. P., & Hounslow, M. (2004). Growth and aggregation of vaterite in seeded-batch experiments. AIChE Journal, 50, 2772–2782.

Bachmeier, K. L., Williams, A. E., Warmington, J. R., & Bang, S. S., (2002). Urease activity in microbiologically-induced calcite precipitation. Journal of Biotechnology, 93 (2), 171–81.

Bang, S. S., & Ramakrishman, V. (2002). Microbial application in strengthening of sandy sub-bases and in remediation of concrete cracks, proposal submitted to National Research Council, USA.

Bang, S. S., Galinat, J. K., & Ramakrishnan, V. (2001). Calcite precipitation induced by polyurethane-immobilized Bacillus pasteurii. Enzyme & Microbial Technology, 28, 404–409.

Bosak, T. & Newman, D. K. (2005). Microbial kinetic controls on calcite morphology in supersaturated solutions. Journal of Sedimentary Research, 75, 190–199.

Bosak, T., Souza-Egipsy, V., Corsettiand, F. A., & Newman, D. K. (2004). Micrometer-scale porosity as a biosignature in carbonate crusts. Geol., , vol. 32, pp. 781–784.

Boquet, E., Boronat, A., & Ramos-Cormenzana, A. (1973). Production of calcite (calcium carbonate) crystals by syoil bacteria in a general phenomenon. Nature, 246, 527–529.

Braissant, O., Cailleau, G., Dupraz, C., & Verrecchia, E. P. (2003). Bacterially induced mineralization of calcium carbonate in tterrestrial environments: the role of exopolysaccharides and amino acids. Journal of Sedimentary Research, 73, 485–490.

Dittrich, M., Müller, B., Mavrocordatos, D., & Wehrli, B. (2003). Induced calcite precipitation by Cyanobacterium Synechococcus. Acta Hydrochimica et Hydrobiologica, 31, 162–169.

Donners, J. J. J. M., Heywood, B. R., Meijer, E. W., Nolte, R. J. M., & Sommerdijk, N. A. J. M. (2002). Control over calcium carbonate phase formation by dendrimer/surfactant templates. Chemistry- A European Journal, 8(11), 2561–2567.

Ferris, F. G., Phoenix, V., Fujita, Y., & Smith, R. W. (2004). Kinetics of calcite precipitation induced by ureolytic bacteria at 10 to 20^{o}c in artificial groundwater. Geochimica et Cosmochimica Acta., 68(8), 1701–1710.

González-Muñoz, M. T., Chekroum, K. B., Aboud, A., Arias, J. M., & Rodriquez-Gallego, M., (2000). Bacterially induced mg-calcite formation: role of mg^{2+} in development of crystal morphology. Journal of Sedimentary Research, 70, 559–564.

Guo, Y., Yang, L., Yang, X., Zhang, X., Zhu, S., & Jiang, K. (2003). Effect of self-assembly of sodium acrylate on the crystallization of calcium carbonate. Macromolec. Biosci., 3, 163–168.

Hammes, F., & Verstraete, W. (2002). Key roles of ph and calcium metabolism in microbial carbonate precipitation. Re/Views in Environmental Science and Bio/Technology, 1, 3-7.

Holt, J. G., Kried, N. R., Senath, P. H. A., Staley, J. T., & Williams, S. T. (1993). Bergey's Manual of Determinative Bacteriology: Philadelphia, Lippincott: Williams and Wikins, , pp. 787.

Longdon, C., Tkahashi, T., Sweeney, C., Chipman, D., Goddard, J., Marubini, F., Aceves, H., Barnett, H., & Atknson, M. J. (2000). Effect of calcium carbonate saturation state on the calcification rate of an experimental coral reef. Global Biogeochemical Cycles, 14(2), 639–654.

Mitchell, A., & Ferris, F. (2006). The Influence of Bacillus pasteurii on the Nucleation and growth of calcium Carbonate. Geomicrobiology Journal, 23, 213–226.

Muyzer, G., de Waal, E. C., & Uitterlinden, A. G. (1993). Profiling of complex microbial populations by denaturing gradient gel electrophoresis analysis of polymerase chain

reaction-amplified genes coding for 16S rRNA. Applied Environmental Microbiology, 59, 695–700.

Ogino, T., Suzuki, T., and Sawada, K. (1987). The formation and transformation mechanism of calcium carbonate in water. Geochimica et Cosmochimica Acta, 51, 2757–2767.

Rivadeneyra, M. A., Ramos-Cormenzana, A., Delgado, G., & Delgado, R. (1996). Process of carbonate precipitation by Deleya halophila. Current Microbiology, 32, 308–313.

Sanchez-Moral, S., Canaveras, J. C., Laiz, L., Saiz-Jimenez, C., Bedoya, J., & Luque, L. (2003). Biomediated precipitation of calcium carbonate metastable phases in hypogean environments: A short review, Geomicrobiology Journal, 20(5), 491–500.

Söllner, C., Burghammer, M., Busch-Nentwich, E., & Berger, G. (2003). Control of crystal size and lattice formation by starmaker in otolith biomineralization. Science, 302, 282–286.

Suckhorukov, G. B., Volodkin, D. V., Günther, A. M., Petrov, A. I., Shenoy, D. B., & Möhwald, H. (2004). Porous calcium carbonate microparticles as templates for encapsulation of bioactive compounds. Journal of Materials Chemistry, 14(7), 2073–2081.

Tai, C. Y., & Chen, F. B. (1998). Polymorphism of $CaCO_3$ precipitated in a constant-composition environment. AIChE Journal, 44, 1790–1798.

Wang, C., He, C., Tong, Z., Liu, X., Ren, B., and Zeng, F., Combination of Adsorption by Porous $CaCO_3$ Microparticles and Encapsulation by Polyelectrolyte Multilayer Films for Sustained Drug delivery. Inter. J. Pharm., 2006, vol. 308, pp. 160–167.

Warren, L. A., Maurice, P. A., Parmar, N., & Ferris, F. G. (2001). Microbially mediated calcium carbonate precipitation: implications for interpreting calcite precipitation and for solid-phase capture of inorganic contaminants. Geomicrobiology Journal, 18, 93–115.

Whiffin, V.S. (2004). Microbial $CaCO_3$ precipitation for the production of biocement. Ph.D dissertation. Murdoch University, Western Australia.

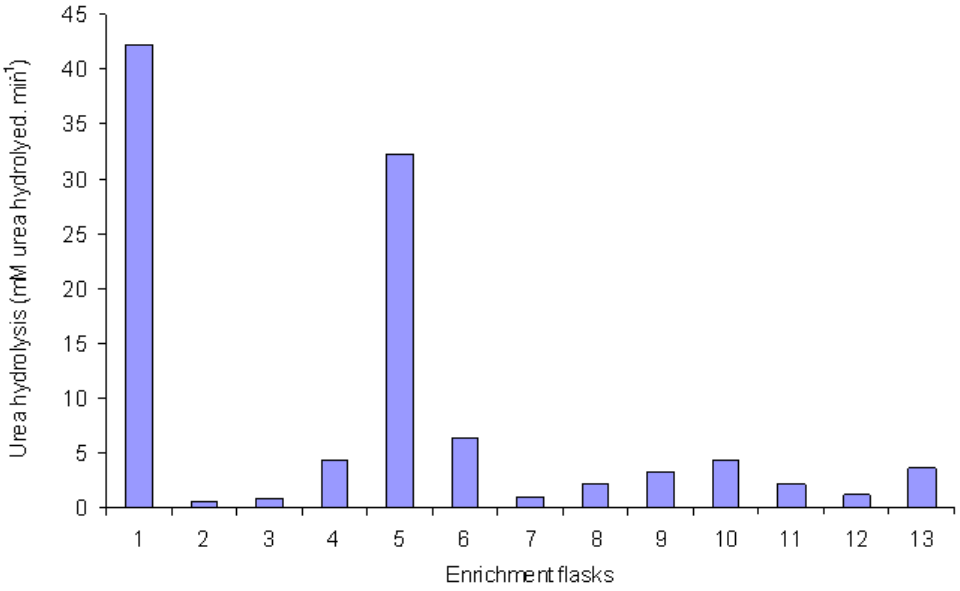

Appendix A: Urease activity of the enrichments incubated for 36-48 hours, at pH 9.0 and 28°C. Yeast extract medium was used (10 $g.L^{-1}$) in the presence of filter sterilized urea (1-5 M) and 1 g soil or sludge.

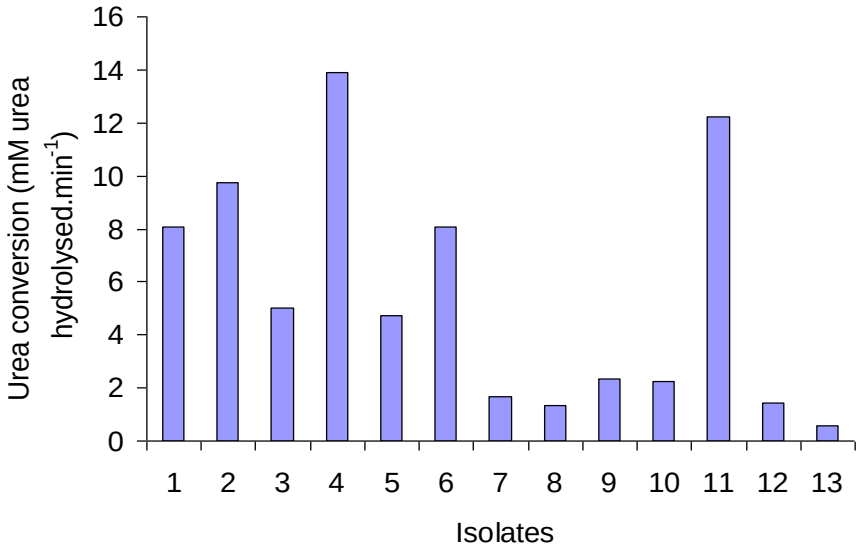

Appendix B: Urease activity measurement by conductivity of the isolated ureolytic strains (1-13) from 13 enrichment cultures in Appendix 1.